

SpanTrain: Highly Efficient Cross-domain Model Distributed Training System under Heterogeneous GPUs and Networks in CEE Environment

Jinquan Wang*
Xiaojuan Liao*
derekjqwang@buaa.edu.cn
liaoxj@buaa.edu.cn
Beihang University
Haidian, Beijing, China

Xuzhao Liu
Beihang University
Haidian, Beijing, China
liuxuzhao@buaa.edu.cn

JiaShun Suo
Beihang University
Haidian, Beijing, China
suojiashun@foxmail.com

Zhisheng Huo†
Beihang University
Haidian, Beijing, China
huozhisheng1122@126.com

Chenhao Zhang
Beihang University
Haidian, Beijing, China
zch13021728086@buaa.edu.cn

Xiangrong Xu
Beihang University
Haidian, Beijing, China
2037369569@qq.com

Runnan Shen
Beihang University
Haidian, Beijing, China
shennr@buaa.edu.cn

Xilong Xie
Beihang University
Haidian, Beijing, China
xxl1399@buaa.edu.cn

Limin Xiao†
Beihang University
Haidian, Beijing, China
xiaolm@buaa.edu.cn

Abstract

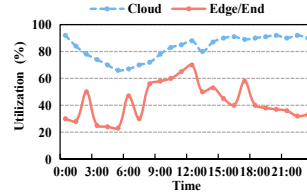
Most existing training systems focus on a single region. In contrast, we envision that cross-region training offers more flexible GPU resource allocation and yields significant potential. However, the hierarchical cluster topology and unstable networks in the cloud-edge-end (CEE) environment, a typical cross-region scenario, pose substantial challenges to building an efficient and autonomous model training system. We propose SpanTrain, a geo-distributed model training system tailored for heterogeneous GPUs and networks in CEE environments. SpanTrain adopts a communication-centric design philosophy to tackle challenges arising from slow and unstable inter-region networks. It begins with a heterogeneous device profiler that identifies and groups devices based on both network and compute characteristics. Leveraging device groups, SpanTrain implements compact, zero-bubble pipeline parallelism, automatically deriving optimal parallel strategies. To further adapt to runtime variability, SpanTrain integrates a dynamic environment adapter that reacts to network fluctuations. Extensive evaluations demonstrate that SpanTrain achieves 1.3-2.8 \times higher training throughput compared to widely used and SOTA training systems.

1 Introduction

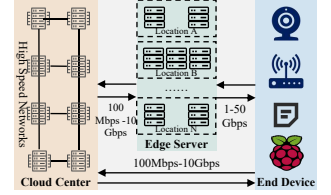
The advancement of AI technology [6, 12, 13, 16, 36, 45, 55] is driving progress across various industries [7, 29, 57], with model training being one of the most critical components. Traditionally, model training is conducted within a single

*Both authors contributed equally to this research.

†Corresponding author.



(a) The workload of the cloud data-center and the edge/end within 24 hours in real world [24, 58].



(b) The CEE environment, a typical cross-region scenario.

Figure 1. The CEE environment and its workload status.

cloud data center. However, we envision that cross-region distributed training [26, 76] will become a key direction for reducing both the barriers and costs associated with model training [1, 30, 61, 64], for the following reasons.

First, as model sizes continue to grow, the demand for GPUs is also increasing [15, 52, 77]. Training tasks cannot be executed immediately [50, 53, 56] when GPUs in a cloud data center are fully utilized. We observe this phenomenon in real-world production environments (Figure 1a): the daily load of a cloud datacenter can reach as high as 78%, with more than 14 hours a day operating above 90%.

Second, physical constraints such as land availability, power consumption, and energy supply are making it increasingly difficult to expand a single cloud data center [41, 52]. As a result, the mainstream approach has shifted toward deploying multiple cloud and edge data centers, with some end devices equipped with GPU resources (e.g., Nvidia P4 [40], RTX 3000 series [39], RTX 4000 series [38], and Cambrian MLU 200 [69] etc.) However, we observe that edge-side

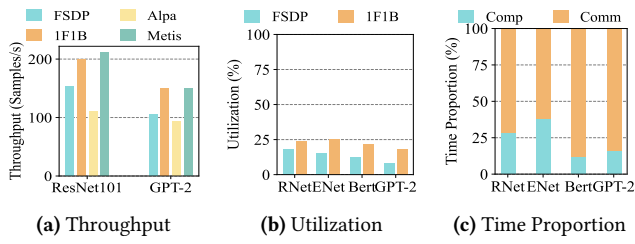


Figure 2. Performance comparison of different methods in a real CEE environment.

computing capabilities remain significantly underutilized, with average GPU utilization rates as low as 28% [17, 64]. This presents a promising opportunity to harness idle GPU resources at the edge for model training.

Third, with the continuous advancement of networking technologies, the bandwidth between different regions has significantly increased, making efficient cross-region model training increasingly feasible. As shown in Figure 1b, the cloud center, edge server and end device are connected by high-speed WANs whose bandwidth is between 100Mbps to 10Gbps [3, 5, 22, 59]. We refer to this environment formed by high-speed networks [10, 51, 70] and heterogeneous computing resources as the CEE environment.

Despite its strong potential, cross-region training still encounters significant technical challenges related to automation and efficiency. We start by directly extending existing training frameworks to the CEE environment. As shown in Figure 2a, we first apply commonly used training frameworks such as PyTorch FSDP [23, 72] and DeepSpeed 1F1B [32, 48] to cross-region training. However, we observe that the training throughput was significantly lower than that of single-region training, with excessive pipeline bubbles leading to GPU utilization falling below 25.6% (Figure 2b).

We further deploy state-of-the-art training frameworks (e.g., Alpa [74], Metis [54]) that can automatically generate training strategies suitable for the heterogeneous devices in CEE environments. However, we observe that these frameworks still fail to fully utilize available GPU resources, with training throughput significant declining. Worse still, the execution plan generation process in some systems (e.g., Asteroid [64]) introduces substantial time overhead, ultimately prolonging the overall training duration. These findings suggest that existing training frameworks fall short in effectively leveraging the aggregated computing capabilities across the CEE environment.

Through in-depth analysis (§2), we identify the root cause as the excessive communication overhead (Figure 2c), which could not be effectively overlapped with computation. This issue stems from two unique characteristics of the CEE environment. First, the environment features a hierarchical cluster topology composed of highly heterogeneous networks and GPUs. As shown in Figure 1b, in addition to high-speed RDMA networks within cloud data centers, the CEE

Table 1. Heterogeneous GPU deployment in Alibaba Cloud and common GPU distribution patterns within edge servers and end devices.

Region	P100	A10	V100	P4	RTX4000	RTX3000
Qingdao Cloud	✗	✗	✓	✓	✗	✗
Beijing Cloud	✓	✓	✓	✓	✗	✗
Hohhot Cloud	✓	✗	✗	✗	✗	✗
Edge Server	✗	✗	✗	✓	✓	✗
End Device	✗	✗	✗	✗	✓	✓

Table 2. Specifications of heterogeneous GPUs capabilities, including computing, memory, and power consumption.

GPU	FP16 (TFLOPs)	FP32 (TFLOPs)	Memory (GB)	Bandwidth (GB/s)	Power (W)
P100	18.7	9.3	16	732	250
A10	62.4	31.2	24	600	150
A100	312	156	40	1555	400
P4	5.5	/	8	192	75
RTX4090	82.58	41.2	24	1018	425
RTX3090	71.16	35.58	24	936.2	350
RTX3080	59.54	29.77	10	760	320

environment includes high-speed LANs connecting edge servers and relatively slow WANs bridging cloud centers, edge clusters, and end devices. The average bandwidth of these WANs varies significantly across segments, resulting in a complex network topology that is largely overlooked by existing training frameworks. Moreover, the heterogeneity of GPU resources in the CEE environment is even more pronounced. Table 1 and Table 2 summarize the GPU configurations across the cross-region setup, encompassing at least 7 different GPU models. These GPUs differ substantially in terms of compute capabilities, memory capacity and bandwidth, making it even more challenging to generate optimal parallelization strategies automatically.

Second, in the CEE environment, training tasks must contend with other workloads (e.g., bursty tasks and routine data transfers [60, 62, 67, 75]) for cross-region network resources, resulting in bandwidth fluctuations and network instability during training. Our experimental results using real-world workloads demonstrate that merely launching a large data transfer task during training can cause resource contention, reducing throughput by over 56% (details in Figure 12b). Current training frameworks fail to adapt to dynamic network bandwidth conditions, thus preventing efficient training in the CEE environment.

We present SpanTrain (§3), a geo-distributed model training system that can automatically generate parallel strategies and adapt to network fluctuations in the CEE environment. The core idea of SpanTrain is network-centric automatic parallel strategy generation and adjustment. While most existing work focuses on the impact of compute heterogeneity

on parallel strategies, in CEE environments, network heterogeneity becomes the primary factor affecting training efficiency. This makes it difficult for existing approaches to fully utilize GPU compute resources across regions. SpanTrain introduces a network-centric approach, prioritizing the mitigation of pipeline bubbles caused by cross-region networks in device grouping, automatic parallel strategy generation, and the adjustment of pipeline stages during execution. Specifically, SpanTrain includes the following three key techniques.

First, SpanTrain introduces the Heterogeneous Devices Profiler, which plans a two-level device grouping before training begins. The first-level groups GPUs based on network performance, eliminating the impact of cross-region network hierarchies on parallel training strategies. The second level further groups GPUs within each network-isolated group based on compute capability, clustering GPUs with similar computation and memory access performance.

Second, SpanTrain proposes the Parallel Strategy Planner, which adopts different parallel strategies for each level of the two-level device group. At the first level, considering the low bandwidth and variability of cross-region networks, SpanTrain introduces compact zero-bubble pipeline parallelism, where weight computations during back propagation are decoupled and inserted into potential pipeline bubbles in a compact fashion. At the second level, SpanTrain automatically generates the optimal combination of pipeline, data and tensor parallelism by jointly considering differences in compute and memory access capabilities across GPUs.

Third, SpanTrain introduces the Dynamic Environment Adapter to cope with network fluctuations. Unlike existing methods that rely on checkpoints and pipeline restarts, SpanTrain monitors network variability and adapts the system through micro-batch-level adjustments, enabling continuous and efficient training without interruptions.

We implement SpanTrain based on PyTorch with around 15K lines of code. We evaluate SpanTrain against a wide range of state-of-the-art training systems including PyTorch DDP [23], PyTorch FSDP [72], DeepSpeed ZeRO2 [44], DeepSpeed Pipeline [37], Gpipe [14], Alpa [74], Metis [54], HetPipe [54], and Asteroid [64]. Extensive results (§4) in a simulated CEE environment show that the SpanTrain outperforms existing distributed training systems by 1.3-2.8 \times in terms of training throughput. Furthermore, under dynamic network changes, SpanTrain improves training throughput by 1.5-1.7 \times compared to existing systems.

In summary, we make the following contribution:

- We analyze the potential benefits and challenges of extending model training to CEE computing environments.
- We propose SpanTrain, a geo-distributed training system designed specifically for CEE computing environments, with a network-centric design philosophy at its core.
- We implement SpanTrain based on PyTorch and conduct extensive evaluations to verify its effectiveness.

2 Background and Motivation

As shown earlier in §1 and Figure 2, existing model training frameworks fail to efficiently utilize computing resources in the CEE environment. In this section, we provide a detailed analysis of the underlying inefficiencies through concrete examples. Our analysis focuses on two primary challenges arising from cross-region deployment: hierarchical cluster topology (§2.1) and network fluctuations (§2.2).

2.1 Challenges 1: Hierarchical Cluster Topology

As noted in §1, CEE environments involve a mix of network types, including relatively slow WANs. Given this, network efficiency becomes an important consideration when designing model training systems. Among the commonly used strategies, Data Parallelism (DP), Tensor Parallelism (TP), and Pipeline Parallelism (PP), TP typically incurs the highest communication overhead [2, 8, 19, 21, 25, 37, 42, 47], and may be less favourable in bandwidth-constrained scenarios. Therefore, we narrow our focus to DP and PP as potentially more suitable options for CEE environments. To explore their efficiency in CEE environments, we begin by analyzing traditional DP (Figure 3a) and 1F1B PP (Figure 3b).

Figure 3a illustrates common issues in DP model training across heterogeneous network in the CEE environment. GPU1 and GPU2 represent two GPU devices with different computing capabilities, located in cloud and edge clusters, respectively. Under synchronous training (e.g., DDP [23], FSDP [72], ZeRO [44]), although these two GPUs have different computational speeds, both of them can complete the computation process quickly. However, after each training epoch, they must rely on slow cross-region network for synchronization. This causes communication time to occupy a significant portion of the total training time, limiting training throughput. Under asynchronous training (e.g., Megatron [48], MindSpore [9]), GPU1 can proceed to the next epoch without waiting for weight synchronization. However, to maintain model convergence, asynchronous updates are typically limited to being at most one epoch ahead. When the cross-region communication time is too large compared to the computing time, even the next epoch of training cannot overlap with communication, resulting in prolonged waiting periods that reduce efficiency.

As shown in Figure 3b, when implementing pipeline parallelism (e.g., HetPipe [42], Asteroid [64], AutoSF [63], FT-PipeHD [4], Metis [54]) across regions, the slowest network link becomes the critical bottleneck that severely limits training throughput. In this scenario, GPU1-GPU2 and GPU3-GPU4 pairs enjoy high-speed connections (e.g., RDMA/LAN), while GPU2-GPU3 suffers from low-speed connections (e.g., WAN). When GPU3 completes micro-batch #0's computing and transfers activations to GPU4, GPU2 simultaneously finishes micro-batch #1, but cannot promptly transfer its activations to GPU3 due to the network bottleneck. This forces

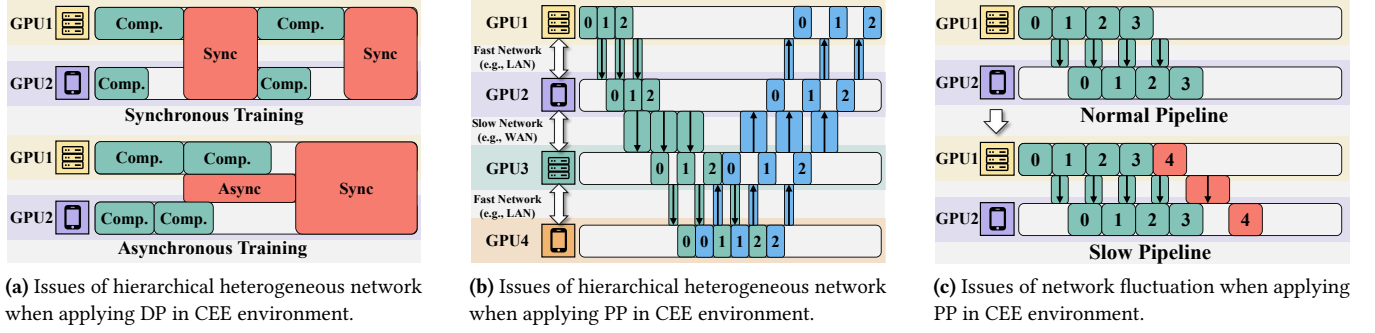


Figure 3. In the CEE environment, current distributed training strategies face two challenges. The hierarchical cluster topology fundamentally constrains training throughput in the CEE environment, while network fluctuations frequently triggers abrupt performance degradation.

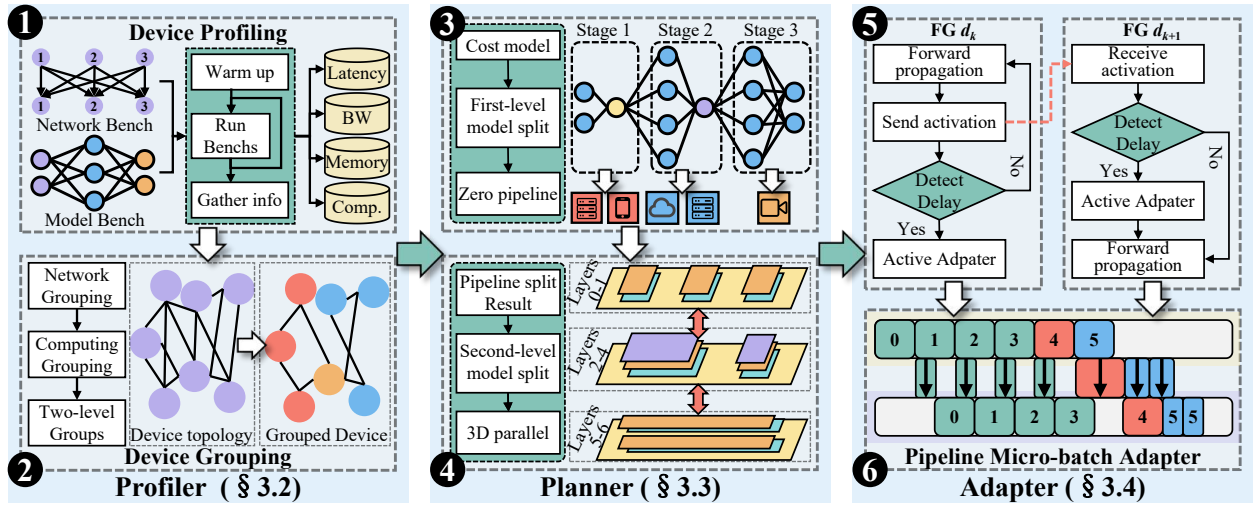


Figure 4. The main working components and workflow of SpanTrain. SpanTrain includes the pre-run performance evaluation component *Heterogeneous Devices Profiler*, the pre-run parallel planning component *Parallel Strategy Planner*, and the runtime environment adaptation component *Dynamic Environment Adapter*.

GPU3 into an idle state, resulting in unavoidable pipeline bubbles. The same issue arises during backward propagation, negatively impacting the utilization of devices connected by high-speed networks (GPU1 / GPU2) and ultimately degrading the pipeline's efficiency. The training performance is constrained by the slowest cross-region connection, exemplifying the "weakest link" problem.

Worse still, the computing heterogeneity (Tables 1 and 2) inherent in CEE environments further exacerbates the inefficiencies of traditional DP and PP caused by slow and heterogeneous networks.

Based on the above analysis, we conclude that both traditional DP and PP suffer from significant efficiency issues in cross-region CEE environments. However, we also observe that, compared to DP, the GPU bubbles in PP are more amenable to mitigation through pipeline optimization.

2.2 Challenges 2: Network Fluctuations

Network fluctuations are common in the CEE environment. For example, multiple edge servers and end devices share uplinks to cloud datacenter. But, bursty traffic patterns, including periodic data reporting and inference result transmission, can suddenly dominate available bandwidth, resulting severe network fluctuations for training task. Prior work [14, 23, 32, 72] is primarily designed for data center networks, under the assumption of relatively stable bandwidth. Consequently, these approaches are ill-suited to handle the dynamic and unpredictable network conditions typical of the CEE environment.

Considering that pipeline parallelism imposes the least demand on network bandwidth among training parallelism techniques, we use a pipeline training example to demonstrate how network fluctuation degrades cross-region training efficiency. In Figure 3c, GPU1 and GPU2 each handle one pipeline stage. Under stable network conditions ("Normal Pipeline" in Figure 3c), computation fully overlaps with

communication, creating a tightly packed pipeline. However, when network bandwidth between GPU1 and GPU2 fluctuates and drops, communication delays can no longer be hidden by computation. When GPU1 completes micro-batch #4 (red block), the activation transfer to GPU2 fails to finish during GPU3's computing of micro-batch #3 ("Slow Pipeline" in Figure 3c). This forces GPU2 and downstream stages into idle states, significantly reducing hardware utilization. Current pipeline systems lack adaptive mechanisms for such scenarios, remaining passive until network conditions recover, which often leads to prolonged throughput degradation during network fluctuations.

Existing approaches (e.g., AutoSF [63]) employ checkpoint-based mechanisms to handle network fluctuations in CEE environments, require restarting the entire pipeline, which incurs prohibitive costs and significant reaction latency.

3 SpanTrain: Design and Implementation

We present SpanTrain, a cross-region model training system designed to address the unique challenges of the CEE environment, as discussed in §2. This section first provides an overview (§ 3.1) and highlights the core idea behind SpanTrain, then delves into the key techniques, namely *Heterogeneous Devices Profiler* (§ 3.2), *Parallel Strategy Planner* (§ 3.3), and *Dynamic Environment Adapter* (§ 3.4).

3.1 Key Idea and Overview

Departing from the compute-centric approach of existing model training systems, SpanTrain generates and adapts parallelization strategies driven by network performance. In the CEE environment, where the cluster topology exhibits a hierarchical characteristic in terms of computing device and network, in addition, network performance also varies significantly across different tiers and exhibits noticeable fluctuations (as shown in §2). Existing systems often mistakenly group cross-region devices into a single device group, resulting in suboptimal parallelization strategies and increased pipeline bubbles during network fluctuations. By treating network performance evaluation as a first-class citizen, SpanTrain effectively addresses the network challenges inherent in cross-region training, with employing computing device performance evaluation as a second-class citizen.

Figure 4 presents the overview and workflow of SpanTrain. SpanTrain first employs the Profiler (§3.2) to find optimal device groups. It then uses the Planner (§3.3) to automatically generate an asymmetric hybrid parallel strategy. Finally, during periods of network fluctuation, it introduces Adapter (§3.4) to mitigate pipeline bubbles, thereby ensuring stable training performance. Specifically, the core components of SpanTrain are as follows:

- *Heterogeneous Devices Profiler* (§ 3.2). It performs lightweight, end-to-end performance profiling of heterogeneous computing devices and networks. Based on the

profiling results (e.g., network latency and bandwidth), it runs a device grouping algorithm to construct a two-level hierarchy: a first-level network device group and a second-level computing device group. Notably, the first-level network device group is carefully designed to address the challenges of cross-region network environments.

- *Parallel Strategy Planner* (§ 3.3). It introduces an asymmetric hybrid parallel mechanism based on the two-level device group. Among various training parallelism strategies, pipeline parallelism offers the lowest network overhead, making it the preferred choice for communication across the first-level device groups in SpanTrain. Given the slow cross-region networks, conventional 1F1B (one-forward-one-backward) pipeline execution introduces significant pipeline bubbles, resulting in suboptimal compute utilization. To alleviate this inefficiency, SpanTrain adopts zero pipeline [43], which separates weight computations during backpropagation and fills idle execution slots, thereby improving compute resource utilization under slow network conditions. In the second-level device group, SpanTrain autonomously derives a 3D parallelism strategy guided by the principle of load balancing across heterogeneous compute resources. This involves sequentially searching for the optimal combination of pipeline, data, and tensor parallelism.
- *Dynamic Environment Adapter* (§3.4). It continuously monitors fluctuations in network performance. Upon detecting significant network-induced delay, e.g., when a later pipeline stage is stalled while waiting for activations, it activates a dynamic micro-batch adjustment mechanism. This mechanism reduces the micro-batch size of the preceding pipeline stage, enabling the subsequent stage to commence computation earlier and thereby enhancing pipeline utilization.

3.2 Heterogeneous Devices Profiler

As discussed in § 2.1, CEE exhibits distinct hierarchical cluster topology where significant variations exist in both network and device across regions. Our observations reveal that inter-region network performance govern cross-region training performance, often becoming the critical bottleneck. To address this issue, *Profiler* automatically generate two-level device groups using a performance evaluation mechanism and a two-level device grouping mechanism.

3.2.1 The Performance Evaluation Mechanism. *Profiler* initiates network performance evaluation by assessing bandwidth and latency between all device pairs. Specifically, *Profiler* generates two distinct test packets: (1) a large payload \mathbb{P}_b sized according to each device's GPU memory capacity for bandwidth measurement, and (2) a minimal payload \mathbb{P}_l containing just five *int32* values for latency profiling. Then, *Profiler* performs multi-round network warmup using payload \mathbb{P}_b . Upon completion, *Profiler* executes CCL primitives

(e.g., AllReduce or broadcast) to repeatedly transfer both \mathbb{P}_b and \mathbb{P}_l , recording their average transfer times as α and β respectively. These metrics are combined through the formula $p_t = \alpha + \beta/m$ to quantify the communication capability between any device pair, where m represents \mathbb{P}_b 's size, establishing a unified performance metric that accounts for both bandwidth and latency characteristics.

Next, *Profiler* executes lightweight model benchmarks comprising diverse neural network architectures (e.g., CNN, Transformer, MLP) and mixed-precision matrix operations to assess heterogeneous devices' computing capabilities. Benchmarks are run repeatedly, recorded average execution time t_i for each task. Subsequently, *Profiler* calculates each device's computing capacity using the formula $p_c = \sum_i (\frac{w_i}{t_i})$, where w represents task-specific weights, quantifying its overall processing capability for parallel workload assignment.

3.2.2 The Two-level Device Grouping Mechanism. Departing from prior cross-region approaches that group devices at node-level granularity, *Profiler* implements a device-level fine-grained GPU grouping mechanism akin to data center practices. *Profiler* performs hierarchical clustering based on network capabilities to establish first-level network device groups, adapting CEE's hierarchical cluster topology. Initially, each device is treated as an independent group, with inter-device communication metrics stored in a max-heap v_n . The first-level network device group algorithm then iteratively (1) extracts the top element from v_n to identify candidate groups, (2) merges groups if the difference between their network capability values is below a predefined threshold, and (3) updates v_n by incorporating new group and computing their average network metrics, gradually constructing CEE's cross-region topology through network-aware aggregation. Notably, *Profiler* retains only the top-level groupings after clustering, discarding intermediate subgroups formed during the algorithm process. As shown in Figure 5, this approach partitioned 12 devices into 3 first-level network device group, each exhibiting internally high bandwidth while clearly delineating cross-region boundaries.

Within each first-level network device group, *Profiler* executes a second-level computing device grouping algorithm, similar to the first-level network device group algorithm but optimized for computing capabilities, to further partition devices into compute-homogeneous second-level computing groups. Figure 5 illustrates three representative outcomes: (1) FG1 splits into three subgroups (SG1-3), (2) FG2 maintains all devices as individual compute units, and (3) FG3 forms hybrid groupings with both a subgroup (SG4) and two standalone devices, demonstrating the algorithm's adaptive granularity to heterogeneous compute resources.

3.3 Parallel Strategy Planner

Conventional parallelism strategies are ineffective for CEE environments (§2.1). To address this, SpanTrain introduces

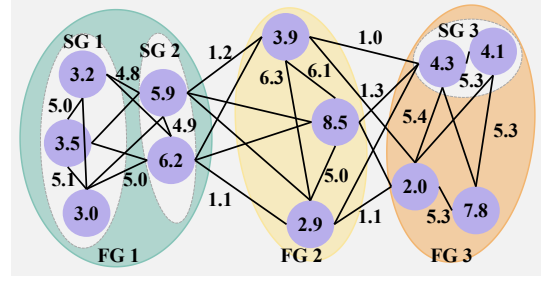
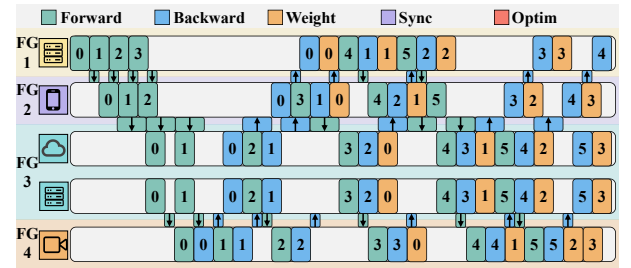
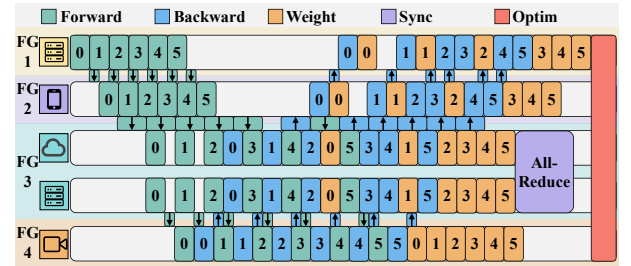


Figure 5. An example of heterogeneous device and network grouping in the CEE environment. (FG: first-level network device group; SG: second-level computing device group)



(a) The original zero-bubble pipeline.



(b) The compact zero-bubble pipeline.

Figure 6. The comparison of original and compact zero-bubble pipeline. (FG: first-level network device group) the *Planner*, which implements a *compact zero-bubble pipeline architecture* that decouples weight updates from gradient computation and proactively inserts the weight updates to pipeline bubbles incurred by the slow and heterogeneous networks whenever feasible. Building upon this foundation, SpanTrain further integrates a region-aware cost model alongside an automated strategy search algorithm to collaboratively generate optimized parallel execution plans.

3.3.1 Compact Zero-bubble Pipeline Architecture. As that pipeline parallelism (PP) incurs the lowest communication overhead, SpanTrain adopts PP across first-level groups. In particular, the *Planner* implements compact zero-bubble PP, building upon the original zero-bubble pipeline design [43], which decouples gradient computation from weight updates. This decoupling substantially enlarges the pipeline scheduling space. However, the original zero-bubble PP assumes that inter-stage communication is faster than both forward and backward propagation computation. This leads

to a rigid execution pattern where forward passes, backward passes, and weight updates follow fixed, non-overlapping phases. Original zero-bubble pipeline generally follows the 1F1B schedule, but it adjusts the starting points of weight update depending on the number of warm-up micro-batches. However, CEE’s hierarchical cluster topology and bandwidth-constrained networks violate its fundamental assumption. As Figure 6a demonstrates, applying the original zero-bubble pipeline to CEE environments exposes critical limitations. Its fixed scheduling pattern generates excessive GPU bubbles that leave most of computing resources idle during network bandwidth-constrained periods.

As shown in Figure 6b, in compact zero-bubble pipeline, there are five operations: forward propagation, backward propagation, weight update, weight synchronization, and optimizer operations. The Planner orchestrates operation execution through the following principle. First, during pipeline warm-up, we greedily execute all available forward propagations, unlike the original zero-bubble pipeline that waits for backward propagation completion before proceeding. This design exploits inter-region network conditions to maximize forward pass throughput, enabling tighter pipeline packing later. As Figure 6a demonstrates, while the original zero-bubble pipeline would delay forward propagation #4 until after FG1’s weight update #0 (creating cascading delays for FG2-FG4). Our compact zero-bubble pipeline completes all six forward passes first. This results denser operation scheduling in downstream stages, reducing total GPU bubbles. Second, we prioritize operations based on their dependency chains: forward propagation (highest), backward propagation (medium), and weight updates (lowest). This hierarchy reflects backward propagation’s dependence on both current and preceding stages’ forward passes, while weight updates only require local gradient completion. As Figure 6b demonstrates in FG2’s execution: after finishing weight update #2, the system immediately processes backward propagations #4 and #5 before completing remaining weight operations. This scheduling strategy triggers FG1’s backward passes earlier, effectively eliminating GPU bubbles in FG1 through proactive dependency resolution. Finally, we employ compact weight update scheduling to exploit all residual GPU bubbles. While prioritized operation scheduling produces tightly-packed pipelines in CEE environment, network performance difference is unavoidable. Our solution dynamically reorganizes weight updates to fill these idle time. As Figure 6b demonstrates in FG3, we insert weight update #0 between backward propagation #2 and forward propagation #5, then immediately resume backward propagation #3 upon its dependency resolution, temporarily suspending non-critical weight updates #1 and #2.

Building atop the pipeline architecture, the *Planner* partitions the model and distributes the resulting segments across first-level groups. Furthermore, it allows heterogeneous parallelism strategies within each first-level network device

group, enabling subdivision into second-level computing device groups based on hardware computing capabilities. This flexibility allows optimal strategy selection (DP, TP, or hybrid) tailored to each second-level group’s specific device characteristics and workload requirements.

3.3.2 Cost Model. To find optimal parallel strategies for CEE environments, SpanTrain first formalizes their costs by Equation 1. It then tries to find a solution that minimizes the following cost (T^*) based on the compact zero-bubble PP.

$$T^* = \min_{s \in \mathbb{S}} \max_{i=1}^P \{ t_i^f + B \cdot t_s^c + \sum_{i=1}^P t_i^l + AL \} \quad (1)$$

$s \in \mathbb{S}$ denotes a specific pipeline stage s within the all stage set \mathbb{S} . P represents s ’s predecessor stages, t_i^f denotes the computation and transfer time between stage i and $i + 1$, and the summation represents the cost of fill stages. B denotes the micro-batch size, t_s^c denotes the computing time per micro-batch in stage s and their product represents the cost of running stages. t_i^l denotes the latency when predecessor stages’ computation fails to fully overlap communication (i.e., synchronization cost). AL is the collective communication time for DP and TP within a first-level network device group.

Stage computing time (t^c and t^f) is derived from the model’s FLOPs requirements normalized by each first-level network device group’s compute capability (obtained from the *Profiler*, §3.2). The residual latency (t_l) quantifies non-overlappable communication as $t^l = t_{comm} - t_{lap}$, where t_{comm} is communication time between two stage and t_{lap} is overlapped communication time (i.e., computing time). Intra-group communication overhead (AL) is modelled as $AL = V / \min(bandwidth)$, where V is communication volume and $\min(bandwidth)$ is lowest bandwidth in a first-level network device group.

The cost model effectively captures training overheads in hierarchical cluster topology, enabling accurate pipeline bubble prediction. This formulation also provides the foundational metrics for our automated search algorithm.

3.3.3 Search Algorithm. Leveraging the pipeline architecture (§3.3.1) and cost model (§3.3.2), we design an automated search algorithm that abstracts CEE’s hierarchical topology, generating near-optimal parallelism strategies.

First-level Network Device Group. As Equation 1 indicates, the *Planner* needs to identify the pipeline stage with the highest cost among the first-level network device groups and seek to minimize it.

The search algorithm 1 explores optimal model splitting within a four-dim space comprising batch size (b), microbatch size (m), model layers, and first-level network device groups. It first enumerates all possible partition combinations for given (\mathbb{B}, \mathbb{S}) configurations (Lines 1-2), then employs beam search to efficiently navigate the subspace of model layers and first-level network device groups. The planner initializes

Algorithm 1: Planner first-level network device group search algorithm.

```

1 foreach  $b \in \mathbb{B}$  do
2   foreach  $m \in \mathbb{M}$  do
3      $\mathbb{A} \leftarrow$  Generate the candidates with length  $l$ ;
4     for  $i = 0; i < \text{max\_iter}; i++$  do
5        $\mathbb{A} \leftarrow$  Expand the candidates;
6       foreach  $a \in \mathbb{A}$  do
7          $T_a^* \leftarrow$  Calculate the current
           optimization goal;
8       Sort the  $\mathbb{A}$  by  $T_a^*$ ;
9        $\mathbb{A} \leftarrow \mathbb{A}[0 : l]$ 
10 return  $\mathbb{A}[0]$ 

```

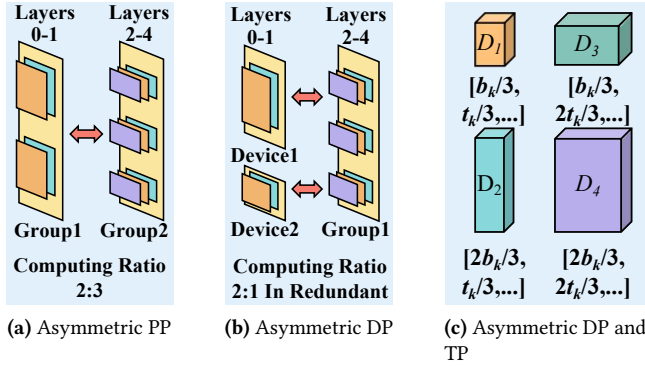


Figure 7. Examples of asymmetric multi-dimensional parallelism. (Group: second-level device group)

by randomly permuting first-level network device groups and generating l candidate split set \mathbb{A} through computing aware model segmentation (Line 3). Through iterative refinement (up to max_iter cycles), it expands the search space by (1) reordering pipeline stages for global exploration and (2) swapping adjacent layers for communication aware local optimization (Line 5). Each candidate split is evaluated via a cost model (Lines 6-7), with the top-1 lowest-cost solutions retained for subsequent iterations (Lines 8-9), progressively converging toward the optimal split strategy.

Second-level Computing Device Group. Within each first-level network device group, we partition the model according to the computing capacity of second-level computing device groups. This is achieved through fully decoupled tensor splitting along the tensor's first and second dimensions, enabling arbitrary proportional allocation across devices to maximize computational resource utilization. Specifically, we designed the following three partitioning strategies:

1) Asymmetric PP. PP is also implemented among second-level device groups. Specifically, *Profiler* can obtain computing capabilities and memory size of second-level computing device group within given first-level network device group. According to the ratio of computing capabilities between

the second-level device groups, the model layers belonging to this stage are further divided into different second-level groups, forming an asymmetric PP. Meanwhile, the standard symmetric TP or DP are implemented within each second-level device group. For example, as shown in Figure 7a, the model layers 0-5 are divided into 2 second-level device groups according to their computing capacity ratio.

2) Asymmetric DP. When PP partitioning encounters a performance bottleneck, such as when a second-level computing device group contains only one device with weak computing power, similar to this type of second-level computing device group, they can collaborate together to compute the same model layer through asymmetric data splitting. For example, as shown in Figure 7b, we divide the 5-layer model into two parts: Group1 is responsible for computing 3 layers, while devices 1 and 2 (the second-level group has only one device) compute 2 layers. Additionally, the input data is split between devices 1 and 2 in a 1:2 ratio to ensure they complete computations simultaneously, thus avoiding the PP computation bottleneck.

3) Asymmetric TP and DP. As mentioned above, among devices more dimension asymmetric TP and DP are supported to achieve that, the tensor and data are divided among devices based on the alignment of the computing capabilities of individual heterogeneous devices to avoid bottleneck nodes. For example, as shown in Figure 7c, the computing capacity ratio of heterogeneous devices is 1 : 2 : 2 : 4, therefore, for a tensor with dimensions of $[b_k, t_k]$, according to this ratio, it is divided into 4 unequal tensors, namely $[b_k/3, t_k/3]$, $[2b_k/3, t_k/3]$, $[b_k/3, 2t_k/3]$, $[2b_k/3, 2t_k/3]$, and which are assigned to corresponding devices, respectively.

3.4 Dynamic Environment Adapter

Network fluctuations in CEE environments introduce additional GPU bubbles throughout the training pipeline (§2.2). To address this issue, the *Adapter* decouples micro-sizes across pipeline stages, enabling independent size adjustment per stage to minimize waiting latency between stages. During network fluctuations, the *Adapter* dynamically adjusts the micro-batch size of affected pipeline stages to enable earlier initiation of subsequent micro-batch processing.

The Adapter comprises two main components: the Forward/Backward Cache and the Forward/Backward Monitor (Figure 8a). Each first-level device group includes a Forward Cache that dynamically adjusts the micro-batch size. The Forward Monitor tracks the available network bandwidth, and based on whether the bandwidth exceeds or falls below a predefined threshold, tensors are either aggregated or re-split for forward propagation. The Backward Cache and Monitor function in a similar manner during back propagation. Together, these components enable dynamic adjustment of micro-batch sizes across first-level device groups.

Specifically, the Adapter adopts the following strategies to adjust the size of micro-batches dynamically. First, to shorten

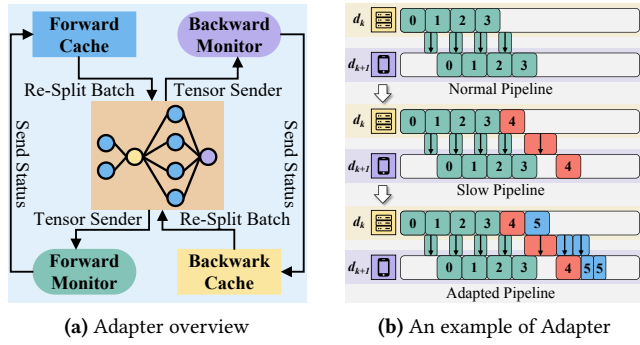


Figure 8. The overview and example of the *Dynamic Environment Adapter*.

the time of the filling stage, the micro-batch size of each first-level device group is reduced when the network capabilities are poor, thus completing the filling as soon as possible.

Second, to reduce the computing bubbles for speeding up the running stage, the Forward and Backward cache monitor the latency taken to send a micro-batch. When they detect a significant transmission delay, the micro-batch size of the current first-level device group is reduced to minimize the waiting time for subsequent groups. For example, as shown in Figure 8b, for the first-level device group d_k , the micro-batch size during the pipeline running process is 32. Upon detecting a transmission delay, the size is reduced to 16, allowing the next device group d_{k+1} to promptly begin its forward propagation.

Third, when the Adapter detects that the forward propagation has been completed entirely, the micro-batch size of all first-level device groups is reduced to accelerate the rest of the backward propagation.

4 Evaluation

We will answer the following questions experimentally: What and why does SpanTrain improve performance compared to the state-of-the-art (SOTA) works in the CEE when training diverse models (§4.2)? What is the effectiveness and adaptation of SpanTrain’s parallel strategy compared to the SOTA works (§4.3 and §4.4)? What is the scalability of SpanTrain compared to the SOTA works (§4.5)? What is the SpanTrain’s system overhead (§4.6)?

4.1 Evaluation Environment

Models and Datasets. We evaluate SpanTrain with 5 typical AI models that are widely used in the CEE, including CV models (i.e., ResNet50, EfficientNet) and NLP models (i.e., Bert-small, GPT-2). We use Cifar-10 dataset with input $3 \times 32 \times 32$ for ResNet101, EfficientNet. For Bert-small, GPT-2, we use the oscar-en-10k dataset with input shape 32×512 .

Environment Setup. We have built a CEE experimental environment configured with 10 servers: 3 servers, each configured with 4 RTX4090 GPUs used as the cloud, 3 servers

with each configured with 2 RTX3090 GPUs used as edge servers, and 4 servers with each configured with 1 RTX3080 GPU used as end devices. In addition, two types of network settings are set up. For Setting 1, the network bandwidth is set to 100 Mbps for the Cloud-Edge and Cloud-End, with the remaining network bandwidth set to 1 Gbps. In Setting 2, all network bandwidth is set to 500 Mbps. Importantly, our method can be extended to the CEE with any resource configuration.

Compared Methods. We compare SpanTrain with both widely-used frameworks and the SOTA methods:

Widely-used Frameworks. We use PyTorch DDP [23], PyTorch FSDP [72], DeepSpeed ZeRO2 [44], DeepSpeed Pipeline [37], and Gpipe [14] as comparison systems for end-to-end performance evaluation.

The SOTA Methods. We use Alpha [74], Metis [54], HetPipe [42], and Asteroid [64] as the SOTA comparison methods for parallel strategies evaluation. Alpha unifies inter-operator and intra-operator parallelism through integer linear programming (ILP) and dynamic programming, achieving optimal model placement for homogeneous clusters. Metis extends Alpha to heterogeneous cloud environments by employing depth first search to identify optimal computation partitions across heterogeneous devices. HetPipe combines data and pipeline parallelism with communication-aware scheduling to maximize throughput on GPU/TPU clusters. Meanwhile, Asteroid specifically targets resource-constrained edge devices, developing a pipeline evaluation method that determines optimal partitions via five dimensional search space exploration. Our evaluation combines established open-source frameworks and custom implementations. Specifically, we employ Alpha’s native JAX implementation for its automated parallelism optimization, while constructing HetPipe’s pipeline mechanism using PyTorch’s distribute package. For Metis and Asteroid, we faithfully reimplement their partition search algorithms while leveraging PyTorch to execute their generated strategies.

4.2 End-to-End Performance Evaluation

This section evaluates the training throughput and time overhead of SpanTrain against widely-used training frameworks in achieving the specified model training accuracy.

Training Throughput. As shown in Figure 9, SpanTrain improves training performance by 2.3-2.38 \times and 1.74-1.85 \times compared to PyTorch DDP in settings 1 and 2, respectively. It achieves 2.05–2.11 \times and 1.61–1.76 \times performance gains compared to PyTorch FSDP in settings 1 and 2, respectively. Similarly, SpanTrain delivers 1.04–1.57 \times and 1.13–1.71 \times performance improvements compared to DeepSpeed Pipeline and Gpipe, respectively. These performance gains are primarily due to SpanTrain’s ability to effectively address device heterogeneity and dynamic network diversity in CEE environments, which are overlooked by both PyTorch DDP, PyTorch

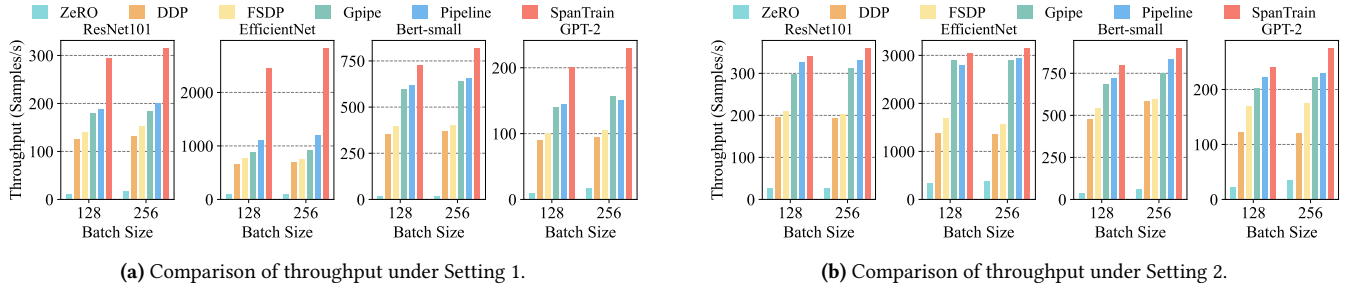


Figure 9. Comparison of throughput for model training using different methods under 2 heterogeneous CEE environment.

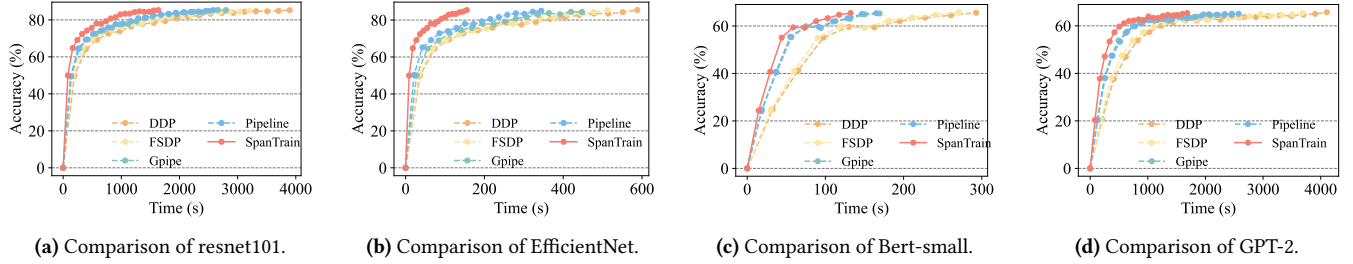


Figure 10. Comparison of model accuracy for model training using different methods under Setting 1.

FDSP, DeepSpeed Pipeline and Gpipe, resulting in worker imbalance and inefficient synchronization. We further observe an intriguing phenomenon in the CEE: larger batch sizes consistently deliver higher throughput. Specifically, our evaluations demonstrate a 6.8-16.2% throughput improvement when increasing batch size from 128 to 256 (Figure 9). This stems from two key factors: (1) longer computing intervals create more opportunities for communication-computation overlap, (2) increased micro-batch counts compress pipeline warm-up phases.

Time Overhead. As shown in Figure 10, the time overhead is evaluated with using different models when achieving the same accuracy in Setting 1. Specifically, training terminates when ResNet-101 and EfficientNet achieve the target accuracy of 85%, and when Bert-small and GPT-2 achieve the target BLEU of 0.65. Compared with existing approaches, SpanTrain takes 55-73.5% less time. This is mainly thanks to SpanTrain can adapt to the CEE by a reasonable hybrid parallel training strategy.

However, although SpanTrain can get better training performance than existing methods, it does not fully translate the training throughput improvement into training acceleration, resulting in the training time increased by 6.4-8.2% in contrast to theoretical improvement. This occurs because our compact zero-bubble pipeline disrupts the conventional weight update sequence, forward and backward no longer strictly operate on the recent model parameters. While such aggressive out-of-order execution improves average throughput by 68.1% (Figure 9), it introduces parameter instability that requires 6.4-8.2% more training iterations to reach target accuracy (Figure 10). Nevertheless, SpanTrain still achieves

faster end-to-end training compared to other approaches, making this trade-off acceptable for most deployments.

4.3 Effectiveness Evaluation of SpanTrain

This section compares SpanTrain with SOTA frameworks, in terms of training throughput and search cost of parallel strategies. We use Setting 1 for evaluation.

4.3.1 Training Throughput. As shown in Figure 11a, when evaluating the training throughput of ResNet, EfficientNet, Bert-small, and GPT-2 using different auto-parallel training frameworks, SpanTrain can outperform existing frameworks in most cases by 1.49-2.85 \times .

Comparison against Alpa. SpanTrain offers 2.46–2.85 \times higher training throughput compared to Alpa. While Alpa pioneered rapid parallel strategy search through unified inter-op/intra-op parallelism, combining tensor, data, and pipeline parallelism via integer linear programming. However, its optimization targets homogeneous clusters (e.g., uniform 8-GPU nodes) and assumes static hardware conditions. This leads to rigid, evenly partitioned model sharding that ignores device heterogeneity and network variance. In contrast, SpanTrain incorporates Profiler that obtains device compute capabilities and network bandwidth, enabling dynamic load balancing adapted to real-time hardware performance.

Comparison against Metis. Our experiments also compare SpanTrain with Metis, a variant of Alpa. While Metis demonstrates measurable throughput improvements over Alpa in our test environment by accounting for device heterogeneity, SpanTrain maintains a 1.49-1.52 \times throughput advantage. This performance gap stems from Metis' simplified heterogeneity model, which only addresses basic inter-cluster differences between two heterogeneous computing

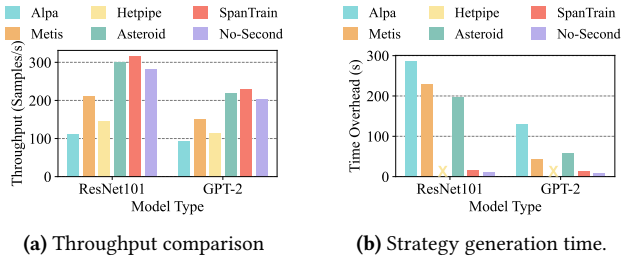


Figure 11. Comparison of different parallel strategy generation methods.

groups while neglecting network diversity and hierarchy. Metis’ sole optimization objective of minimizing inter-cluster communication consequently yields limited performance gains.

Comparison against HetPipe. SpanTrain demonstrates superior training throughput, achieving 2.03-2.18× improvements over HetPipe. HetPipe coordinates heterogeneous devices and diverse networks through communication scheduling. But, its parameter server (PS) architecture necessitates epoch-level weight synchronization that halts training and limits throughput. However, SpanTrain’s fully asynchronous pipeline parallelism eliminates this bottleneck.

Comparsion against Asteroid. SpanTrain achieves 1.04-1.05× higher training throughput than Asteroid. Asteroid uses dynamic programming based multi-dimensional search approach to achieve similar performance. However, SpanTrain’s strategy more comprehensively accounts for the CEE hierarchical structures, avoiding the suboptimal parallel strategy generated by Asteroid’s overcomplexed assumptions. Furthermore, SpanTrain’s significantly faster strategy search enables quicker training initialization, and its dynamic microbatch scheduling combined with asynchronous execution provides additional performance gains beyond Asteroid’s capabilities.

4.3.2 Cost Time. As illustrated in Figure 11b, Alpha, Metis, and Asteroid exhibit substantially longer parallelism strategy search time compared to SpanTrain. Alpha requires 286.3 seconds for ResNet101 and 130 seconds for GPT-2, primarily due to its exhaustive search across all possible device combinations, layer mappings, and hyperparameters (e.g., batch/micro-batch sizes), resulting in an $O(n! \cdot n! \cdot n^2)$ search space. Metis reduces this overhead to 230 seconds (ResNet101) and 43 seconds (GPT-2) by pre-grouping devices into performance, balanced device groups and applying search-space pruning, though it still maintains $O(n! \cdot n^3)$ time complexity. Asteroid further shortens the search time to 197 seconds (ResNet101) and 59 seconds (GPT-2) but remains slower than SpanTrain because it (1) operates on the full device set without pre-grouping and (2) incurs additional latency from runtime memory analysis and parallel strategy evaluation.

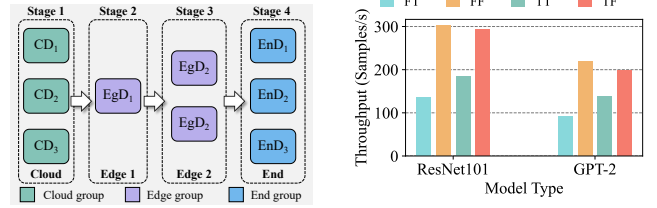


Figure 12. Evaluation results for SpanTrain’s Adapter component.

In contrast, SpanTrain achieves significantly faster strategy discovery through three key optimizations: (1) topology-aware device grouping that reduces the search space to near-constant complexity, (2) rapid candidate generation via pre-defined partitioning points, and (3) lightweight refinement using beam search.

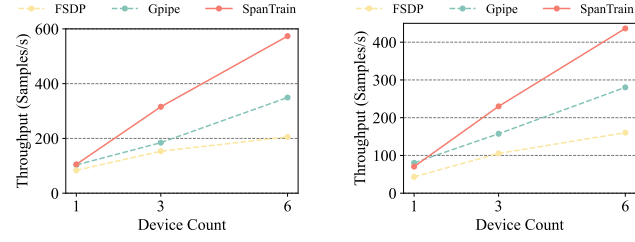
4.3.3 Profit of Second-Level Computing Device Group.

In Figure 11a, we evaluate the training performance when turning off SpanTrain’s model split among second-level device groups (No-Second). The experimental results show that the training performance of No-Second declines by 10.93% and 12.04% compared to SpanTrain when using ResNet101 and GPT-2, respectively. This is due to the inability to fully leverage the resources of the heterogeneous computing devices when model splitting is disabled among second-level device groups. However, its training performance is still higher than existing parallel training frameworks such as Alpha, Metis, and Hetpipe. As shown in Figure 11b, turning off SpanTrain’s second-level device group search can reduce its search time of the parallel strategy by roughly 20%.

4.4 Evaluating SpanTrain’s Adaptation

As shown in Figure 12, with Setting 1, we evaluate the SpanTrain’s adaption in the network fluctuation environment. As shown in Figure 12a, the ResNet101 and GPT-2 models are divided into 4 stages and spread over different 4 first-level network device groups. During our experiments, we add the noise to the network between 4 first-level network device groups, reducing their bandwidth by 40-60%, to emulate the network fluctuation. We evaluate four scenarios formed by two binary conditions: (1) *Adapter* activated or not and (2) network noise added or not. Specifically, including ① with the *Adapter* off and with network bandwidth degradation (FT), ② with the *Adapter* off and without network bandwidth degradation (FF), ③ with the *Adapter* on and with network bandwidth degradation (TT), and ④ with the *Adapter* on and without network bandwidth degradation (TF).

As shown in Figure 12b, the Adaptor can provide high training throughput when facing the dynamic changing of the network. The FT and TT comparison in Figure 12b reveals that *Adapter* improves training throughput by up to 1.35×



(a) Throughput results for varying number of devices with ResNet101. (b) Throughput results for varying number of devices with GPT-2.

Figure 13. Throughput results for varying numbers of devices.

and 1.49× for ResNet101 and GPT-2 during bandwidth fluctuations. This acceleration from its dynamic network-aware optimization: (1) decoupling micro-batch sizes across pipeline stages, and (2) independently adjusting microbatches per stage based on real-time network latency measurements. Under stable network status, our analysis reveals a slight performance decline when enabling Adapter. As shown in Figure 12b, the FF and TF comparison demonstrates throughput reductions of 2.9% (ResNet101) and 9.3% (GPT-2), attributable to two factors: (1) smaller micro-batch sizes decreasing hardware utilization efficiency, and (2) increased protocol overhead from more frequent communication. However, these costs can be accepted, in the whole training process including network fluctuation, Adapter can improve the throughput by 32.1-39.7%, when offsetting its own cost mentioned above.

4.5 Scalability Evaluation

As illustrated in Figure 13, the scalability of SpanTrain is evaluated by examining the model training throughput under varying numbers of devices. Based on the above configuration of the CEE, we ran this experiment by setting the server number of edge and end to be 1, 3, and 6, respectively, with the number of cloud servers being fixed, and using the network Setting 1 configuration described in §4.1. ResNet101 and GPT-2 models are used to be trained, and the batch size is set to be 128.

The experimental results show that SpanTrain’s average training throughput outperforms that of PyTorch-FSDP and GPipe by 2.79× and 1.64×, respectively. That is because PyTorch FSDP requires weight synchronization across multiple nodes, where larger node counts exacerbate communication bottlenecks from stragglers. Meanwhile, GPipe’s 1F1B pipeline structure suffers from cascading inefficiencies: as model stages increase, (1) slow networks affect more stages, and (2) GPU bubble time grows proportionally with device count, significantly limiting throughput growth. In contrast, SpanTrain’s compact zero-bubble pipeline achieves superior scaling by: (1) decoupling weight updates to scheduling, and (2) bubble-padded execution that maximizes device resource

utilization. Our approach reduces GPU idle time and demonstrates better performance scaling with increasing devices compared to existing methods.

4.6 System Overhead

Next, we evaluate SpanTrain’s overhead imposed by the Profiler, Planner, and Adapter components, respectively.

The Overhead of the Profiler. Profiler’s overhead is comprised of two parts. First, there is the overhead originated from network capability evaluation. We employ CCL communication to evaluate network capacities, and in our current experimental setup, one cycle of network evaluation takes 15-33 seconds. When 10 rounds of network evaluation are executed, which takes around 143 seconds. Second, there is another overhead from computing capability evaluation. We use a medium-scale neural network to evaluate computing capability, and fitting functions are utilized to acquire the computing capability of other scale models. In the current configuration, computing capability evaluation takes about 83-159 seconds.

The Overhead of the Planner. The main overhead in Planner is the search overhead for finding the optimal parallel strategy, which has been described in full in §4.3. Specifically, Planner uses a dictionary to cache the results of past searches to accelerate the search process, resulting in an additional storage complexity of $O(n!)$, where n is the number of first-level device groups. The memory overhead of the Planner is marginal, with less than 1 MB through our experimental results.

The Overhead of the Adapter. The primary overhead of Adapter is caused by monitoring network transmission performance and identifying network fluctuations. The Adapter employs timers to monitor network performance, and each timer brings tiny CPU calculation and memory overhead. To detect network bandwidth changes, the time spent on each 20 micro-batch transmission is recorded, so the algorithm with time complexity $O(n)$ is used to determine whether there are any changes, where n is the number of first-level device groups.

Overall, these are shown to be that the time and storage overhead imposed by SpanTrain is lightweight and causes minimal impact in model training.

5 Related Work

There has been extensive research on distributed training in both industry and academia.

Single Datacenter Distributed Training. Model training within a single datacenter has been extensively studied, with parallel strategy [14, 23, 35, 37, 44, 66, 71, 72], hardware-software co-design [27, 33, 46, 61, 68], and fault tolerance for large scale model training [34, 49] being the key research focuses. For example, SmartMoE[66] achieves efficient MoE

parallelism and training, KungFu [27] enables adaptive training in cloud datacenters, and CheckFreq [34] implements fine-grained checkpointing.

Geo-distributed Training. MoDNN [28] and CoEdge [65] divide DNN workloads dynamically based on device computing capabilities, allowing for collaboration with edges. DeepThings [73] uses FTP and distributed work theft techniques to enable collaboration between IoT devices and edge clusters. EDDL [11] and AutoSF [63] adjust to changing edge resources and optimize aggregation structure and frequency. FTPipeHD [4] dynamically optimizes partition locations and presents a weight redistribution mechanism to address the fault issue during training.

Auto Parallel Strategy Generation. Several works, like AMP [20] and Alpa [74], use automated tensor or operator-level parallelism on homogeneous GPUs. Merak [18] and Galvatron [31] can accomplish 3D parallel automation for big fundamental models on homogenous GPUs. Metis [54] automates the design of heterogeneous parallel methods and optimizes them on heterogeneous GPUs with a large parallel strategy search space. Asteroid [64] automatically develops HPP strategies for multi-edge models, allowing for automated training of heterogeneous edge hardware.

6 Conclusion

This paper proposes SpanTrain, a geo-distributed model training system, which is a communication-centric training framework to tackle the issue of slow and unstable inter-region networks in the cross-region training. Specifically, SpanTrain can provide a compact, zero-bubble pipeline parallelism, with automatically deriving optimal parallel strategies, and react to network fluctuations in real time. The experimental results show that SpanTrain can provide an efficient training performance in contrast to the SOTA methods and existing parallel training frameworks in the CEE environment.

References

- [1] Romil Bhardwaj, Zhengxu Xia, Ganesh Ananthanarayanan, Junchen Jiang, Yuanchao Shu, Nikolaos Karianakis, Kevin Hsieh, Paramvir Bahl, and Ion Stoica. 2022. Ekyra: Continuous Learning of Video Analytics Models on Edge Compute Servers. In *19th USENIX Symposium on Networked Systems Design and Implementation (NSDI 22)*. 119–135.
- [2] Zhengda Bian, Qifan Xu, Boxiang Wang, and Yang You. 2021. Maximizing Parallelism in Distributed Training for Huge Neural Networks. <https://doi.org/10.48550/arXiv.2105.14450> arXiv:2105.14450 [cs]
- [3] Imane Cheikh, Rachid Aouami, Essaid Sabir, Mohamed Sadik, and Sébastien Roy. 2022. Multi-Layered Energy Efficiency in LoRa-WAN Networks: A Tutorial. *IEEE Access* 10 (2022), 9198–9231.
- [4] Yuhao Chen, Qianqian Yang, Shibo He, Zhiguo Shi, Jiming Chen, and Mohsen Guizani. 2024. FTPipeHD: A Fault-Tolerant Pipeline-Parallel Distributed Training Approach for Heterogeneous Edge Devices. *IEEE Transactions on Mobile Computing* 23, 4 (April 2024), 3200–3212. <https://doi.org/10.1109/TPDS.2023.3272567>
- [5] Naga Srinivasarao Chilamkurthy, Om Jee Pandey, Anirban Ghosh, Linga Reddy Cenkeramaddi, and Hong-Ning Dai. 2022. Low-Power Wide-Area Networks: A Broad Overview of Its Different Aspects. *IEEE Access* 10 (2022), 81926–81959.
- [6] Zihang Dai, Zhilin Yang, Yiming Yang, Jaime Carbonell, Quoc V. Le, and Ruslan Salakhutdinov. 2019. Transformer-XL: Attentive Language Models Beyond a Fixed-Length Context. <https://arxiv.org/abs/1901.02860v3>.
- [7] Runliang Dou, Guiyu Zhuang, Xin Liu, Yanchao Hou, and Jing Sun. 2024. Potential of AI for Service Performance of Manufacturers: Analytical and Empirical Insights. *Advanced Engineering Informatics* 60 (2024), 102383.
- [8] Shiqing Fan, Yi Rong, Chen Meng, Zongyan Cao, Siyu Wang, Zhen Zheng, Chuan Wu, Guoping Long, Jun Yang, Lixue Xia, Lansong Diao, Xiaoyong Liu, and Wei Lin. 2021. DAPPLE: A Pipelined Data Parallel Approach for Training Large Models. In *Proceedings of the 26th ACM SIGPLAN Symposium on Principles and Practice of Parallel Programming (PPoPP '21)*. Association for Computing Machinery, New York, NY, USA, 431–445. <https://doi.org/10.1145/3437801.3441593>
- [9] MindSpore Group. 2025. MindSpore Official Site | MindSpore. <https://www.mindspore.cn/en>.
- [10] Liangzhe Han, Bowen Du, Leilei Sun, Yanjie Fu, Yisheng Lv, and Hui Xiong. 2021. Dynamic and Multi-faceted Spatio-temporal Deep Learning for Traffic Speed Forecasting. In *Proceedings of the 27th ACM SIGKDD Conference on Knowledge Discovery & Data Mining*. ACM, Virtual Event Singapore, 547–555. <https://doi.org/10.1145/3447548.3467275>
- [11] Pengzhan Hao and Yifan Zhang. 2021. EDDL: A Distributed Deep Learning System for Resource-limited Edge Computing Environment. In *2021 IEEE/ACM Symposium on Edge Computing (SEC)*. 1–13. <https://doi.org/10.1145/3453142.3491286>
- [12] Kaiming He, Xiangyu Zhang, Shaoqing Ren, and Jian Sun. 2016. Deep Residual Learning for Image Recognition. In *Proceedings of the IEEE Conference on Computer Vision and Pattern Recognition*. 770–778.
- [13] Gao Huang, Zhuang Liu, Laurens Van Der Maaten, and Kilian Q. Weinberger. 2017. Densely Connected Convolutional Networks. In *Proceedings of the IEEE Conference on Computer Vision and Pattern Recognition*. 4700–4708.
- [14] Yanping Huang, Youlong Cheng, Ankur Bapna, Orhan Firat, Mia Xu Chen, Dehao Chen, Hyukjoong Lee, Jiquan Ngiam, Quoc V. Le, Yonghui Wu, and Zhifeng Chen. 2019. GPipe: Efficient Training of Giant Neural Networks Using Pipeline Parallelism. <https://doi.org/10.48550/arXiv.1811.06965> arXiv:1811.06965 [cs]
- [15] Ziheng Jiang, Haibin Lin, Yinmin Zhong, Qi Huang, Yangrui Chen, Zhi Zhang, Yanghua Peng, Xiang Li, Cong Xie, Shibiao Nong, Yulu Jia, Sun He, Hongmin Chen, Zhihao Bai, Qi Hou, Shipeng Yan, Ding Zhou, Yiyao Sheng, Zhuo Jiang, Haohan Xu, Haoran Wei, Zhang Zhang, Pengfei Nie, Leqi Zou, Sida Zhao, Liang Xiang, Zherui Liu, Zhe Li, Xiaoying Jia, Jianxi Ye, Xin Jin, and Xin Liu. 2024. MegaScale: Scaling Large Language Model Training to More Than 10,000 GPUs. arXiv:2402.15627 [cs]
- [16] Nikita Kitaev, Łukasz Kaiser, and Anselm Levskaya. 2020. Reformer: The Efficient Transformer. <https://doi.org/10.48550/arXiv.2001.04451> arXiv:2001.04451 [cs]
- [17] Young D. Kwon, Rui Li, Stylianos Venieris, Jagmohan Chauhan, Nicholas Donald Lane, and Cecilia Mascolo. 2024. TinyTrain: Resource-Aware Task-Adaptive Sparse Training of DNNs at the Data-Scarce Edge. In *Forty-First International Conference on Machine Learning*.
- [18] Zhiqian Lai, Shengwei Li, Xudong Tang, Keshi Ge, Weijie Liu, Yabo Duan, Linbo Qiao, and Dongsheng Li. 2023. Merak: An Efficient Distributed DNN Training Framework with Automated 3D Parallelism for Giant Foundation Models. *IEEE Transactions on Parallel and Distributed Systems* 34, 5 (May 2023), 1466–1478. <https://doi.org/10.1109/TPDS.2023.3247001>
- [19] Dmitry Lepikhin, Hyukjoong Lee, Yuanzhong Xu, Dehao Chen, Orhan Firat, Yanping Huang, Maxim Krikun, Noam Shazeer, and

- Zhifeng Chen. 2020. GShard: Scaling Giant Models with Conditional Computation and Automatic Sharding. <https://doi.org/10.48550/arXiv.2006.16668> arXiv:2006.16668 [cs]
- [20] Dacheng Li, Hongyi Wang, Eric Xing, and Hao Zhang. 2022. Amp: Automatically Finding Model Parallel Strategies with Heterogeneity Awareness. *Advances in Neural Information Processing Systems* 35 (2022), 6630–6639.
- [21] Fanxin Li, Shixiong Zhao, Yuhao Qing, Xusheng Chen, Xiuxian Guan, Sen Wang, Gong Zhang, and Heming Cui. 2023. Fold3D: Rethinking and Parallelizing Computational and Communicational Tasks in the Training of Large DNN Models. *IEEE Transactions on Parallel and Distributed Systems* 34, 5 (May 2023), 1432–1449. <https://doi.org/10.1109/TPDS.2023.3247883>
- [22] Ruihan Li, Fangdan Ye, Yifei Yuan, Ruizhen Yang, Bingchuan Tian, Tianchen Guo, Hao Wu, Xiaobo Zhu, Zhongyu Guan, and Qing Ma. 2024. Reasoning about Network Traffic Load Property at Production Scale. In *21st USENIX Symposium on Networked Systems Design and Implementation (NSDI 24)*. 1063–1082.
- [23] Shen Li, Yanli Zhao, Rohan Varma, Omkar Salpekar, Pieter Noordhuis, Teng Li, Adam Paszke, Jeff Smith, Brian Vaughan, Pritam Damania, and Soumith Chintala. 2020. PyTorch Distributed: Experiences on Accelerating Data Parallel Training. *Proceedings of the VLDB Endowment* 13, 12 (Aug. 2020), 3005–3018. <https://doi.org/10.14778/3415478.3415530>
- [24] Yanan Li, Haitao Yuan, Zhe Fu, Xiao Ma, Mengwei Xu, and Shangguang Wang. 2023. ELASTIC: Edge Workload Forecasting Based on Collaborative Cloud-Edge Deep Learning. In *Proceedings of the ACM Web Conference 2023 (WWW '23)*. Association for Computing Machinery, New York, NY, USA, 3056–3066. <https://doi.org/10.1145/3543507.3583436>
- [25] Zhiqi Lin, Youshan Miao, Quanlu Zhang, Fan Yang, Yi Zhu, Cheng Li, Saeed Maleki, Xu Cao, Ning Shang, Yilei Yang, Weijiang Xu, Mao Yang, Lintao Zhang, and Lidong Zhou. 2024. nnScaler: Constraint-Guided Parallelization Plan Generation for Deep Learning Training. In *18th USENIX Symposium on Operating Systems Design and Implementation*.
- [26] Xin Liu, Yaran Chen, Haoran Li, Boyu Li, and Dongbin Zhao. 2025. Cross-Domain Random Pre-training with Prototypes for Reinforcement Learning. <https://doi.org/10.48550/arXiv.2302.05614> arXiv:2302.05614 [cs]
- [27] Luo Mai, Guo Li, Marcel Wagenländer, Konstantinos Fertakis, Andrei-Octavian Brabete, and Peter Pietzuch. [n. d.]. KungFu: Making Training in Distributed Machine Learning Adaptive.
- [28] Jiachen Mao, Xiang Chen, Kent W. Nixon, Christopher Krieger, and Yiran Chen. 2017. MoDNN: Local Distributed Mobile Computing System for Deep Neural Network. In *Design, Automation & Test in Europe Conference & Exhibition (DATE), 2017*. IEEE, Lausanne, Switzerland, 1396–1401. <https://doi.org/10.23919/DATE.2017.7927211>
- [29] Alessio Meloni, Paolo Attilio Pegoraro, Luigi Atzori, Andrea Benigni, and Sara Sulis. 2018. Cloud-Based IoT Solution for State Estimation in Smart Grids: Exploiting Virtualization and Edge-Intelligence Technologies. *Computer Networks* 130 (2018), 156–165.
- [30] Hao Miao, Yan Zhao, Chenjuan Guo, Bin Yang, Kai Zheng, Feiteng Huang, Jiandong Xie, and Christian S. Jensen. 2024. A Unified Replay-Based Continuous Learning Framework for Spatio-Temporal Prediction on Streaming Data. In *2024 IEEE 40th International Conference on Data Engineering (ICDE)*. 1050–1062. <https://doi.org/10.1109/ICDE60146.2024.00085>
- [31] Xupeng Miao, Yujie Wang, Youhe Jiang, Chunan Shi, Xiaonan Nie, Hailin Zhang, and Bin Cui. 2022. Galvaton: Efficient Transformer Training over Multiple GPUs Using Automatic Parallelism. *Proceedings of the VLDB Endowment* 16, 3 (Nov. 2022), 470–479. <https://doi.org/10.14778/3570690.3570697>
- [32] Microsoft. 2024. Microsoft/DeepSpeed: DeepSpeed Is a Deep Learning Optimization Library That Makes Distributed Training and Inference Easy, Efficient, and Effective. <https://github.com/microsoft/DeepSpeed>.
- [33] Zizhao Mo, Huanle Xu, and Chengzhong Xu. 2024. Heet: Accelerating Elastic Training in Heterogeneous Deep Learning Clusters. In *Proceedings of the 29th ACM International Conference on Architectural Support for Programming Languages and Operating Systems, Volume 2 (ASPLOS '24, Vol. 2)*. Association for Computing Machinery, New York, NY, USA, 499–513. <https://doi.org/10.1145/3620665.3640375>
- [34] Jayashree Mohan, Amar Phanishayee, and Vijay Chidambaram. 2021. CheckFreq: Frequent, Fine-Grained DNN Checkpointing. In *Usenix Fast 2021*.
- [35] Jayashree Mohan, Amar Phanishayee, Ashish Raniwala, and Vijay Chidambaram. 2021. Analyzing and Mitigating Data Stalls in DNN Training. In *Vldb 2021*.
- [36] Tsendsuren Munkhdalai, Manaal Faruqi, and Siddharth Gopal. 2024. Leave No Context Behind: Efficient Infinite Context Transformers with Infini-attention. <https://doi.org/10.48550/arXiv.2404.07143> arXiv:2404.07143 [cs]
- [37] Deepak Narayanan, Aaron Harlap, Amar Phanishayee, Vivek Seshadri, Nikhil R. Devanur, Gregory R. Ganger, Phillip B. Gibbons, and Matei Zaharia. 2019. PipeDream: Generalized Pipeline Parallelism for DNN Training. In *Proceedings of the 27th ACM Symposium on Operating Systems Principles (SOSP '19)*. Association for Computing Machinery, New York, NY, USA, 1–15. <https://doi.org/10.1145/3341301.3359646>
- [38] NVIDIA. [n. d.]. GeForce RTX 4090 Graphics Cards for Gaming | NVIDIA. <https://www.nvidia.com/en-us/geforce/graphics-cards/40-series/rtx-4090/>.
- [39] NVIDIA. 2024. NVIDIA GeForce RTX 30 Series GPUs Powered by Ampere Architecture. <https://www.nvidia.com/en-us/geforce/graphics-cards/30-series/>.
- [40] NVIDIA. 2025. TESLA P4 GPU ACCELERATOR. <https://www.nvidia.com/content/dam/en-zz/Solutions/design-visualization/solutions/resources/documents1/Tesla-P4-Product-Brief.pdf>.
- [41] OpenAI. 2024. Multi-Datacenter Training: OpenAI's Ambitious Plan To Beat Google's Infrastructure.
- [42] Jay H. Park, Gyeongchan Yun, Chang M. Yi, Nguyen T. Nguyen, Seungmin Lee, Jaesik Choi, Sam H. Noh, and Young-ri Choi. 2020. {HetPipe}: Enabling Large {DNN} Training on (Whimpy) Heterogeneous {GPU} Clusters through Integration of Pipelined Model Parallelism and Data Parallelism. In *2020 USENIX Annual Technical Conference (USENIX ATC 20)*. 307–321.
- [43] Penghui Qi, Xinyi Wan, Guangxing Huang, and Min Lin. 2023. Zero Bubble Pipeline Parallelism. <https://doi.org/10.48550/arXiv.2401.10241> arXiv:2401.10241 [cs]
- [44] Samyam Rajbhandari, Jeff Rasley, Olatunji Ruwase, and Yuxiong He. 2020. ZeRO: Memory Optimizations Toward Training Trillion Parameter Models. <https://doi.org/10.48550/arXiv.1910.02054> arXiv:1910.02054 [cs]
- [45] J. Redmon. 2016. You Only Look Once: Unified, Real-Time Object Detection. In *Proceedings of the IEEE Conference on Computer Vision and Pattern Recognition*.
- [46] Zhaoyan Shen, Qingxiang Tang, Tianren Zhou, Yuhao Zhang, Zhiping Jia, Dongxiao Yu, Zhiyong Zhang, and Bingzhe Li. 2024. ASHL: An Adaptive Multi-Stage Distributed Deep Learning Training Scheme for Heterogeneous Environments. *IEEE Trans. Comput.* 73, 1 (2024), 30–43. <https://doi.org/10.1109/TC.2023.3315847>
- [47] Mohammad Shoeybi, Mostofa Patwary, Raul Puri, Patrick LeGresley, Jared Casper, and Bryan Catanzaro. 2020. Megatron-LM: Training Multi-Billion Parameter Language Models Using Model Parallelism. <https://doi.org/10.48550/arXiv.1909.08053> arXiv:1909.08053 [cs]
- [48] Shaden Smith, Mostofa Patwary, Brandon Norick, Patrick LeGresley, Samyam Rajbhandari, Jared Casper, Zhun Liu, Shrimai Prabhumoye, George Zerveas, Vijay Korthikanti, Elton Zhang, Rewon Child, Reza Yazdani Aminabadi, Julie Bernauer, Xia Song, Mohammad Shoeybi, Yuxiong He, Michael Houston, Saurabh Tiwary, and Bryan

- Catanzaro. 2022. Using DeepSpeed and Megatron to Train Megatron-Turing NLG 530B, A Large-Scale Generative Language Model. <https://doi.org/10.48550/arXiv.2201.11990> arXiv:2201.11990 [cs]
- [49] Foteini Strati, Michal Friedman, and Ana Klimovic. 2025. PCcheck: Persistent Concurrent Checkpointing for ML. In *Proceedings of the 30th ACM International Conference on Architectural Support for Programming Languages and Operating Systems, Volume 1*. ACM, Rotterdam Netherlands, 811–827. <https://doi.org/10.1145/3669940.3707255>
- [50] Kahou Tam, Chunlin Tian, Li Li, Haikai Zhao, and ChengZhong Xu. 2024. FedHybrid: Breaking the Memory Wall of Federated Learning via Hybrid Tensor Management. In *Proceedings of the 22nd ACM Conference on Embedded Networked Sensor Systems*. ACM, Hangzhou China, 394–408. <https://doi.org/10.1145/3666025.3699346>
- [51] Jiabin Tang, Wei Wei, Lianghao Xia, and Chao Huang. 2024. EasyST: A Simple Framework for Spatio-Temporal Prediction. In *Proceedings of the 33rd ACM International Conference on Information and Knowledge Management*. ACM, Boise ID USA, 2220–2229. <https://doi.org/10.1145/3627673.3679749>
- [52] Gemini Team. 2024. Gemini 1.5: Unlocking Multimodal Understanding across Millions of Tokens of Context. <https://doi.org/10.48550/arXiv.2403.05530> arXiv:2403.05530 [cs]
- [53] Chunlin Tian, Li Li, Kahou Tam, Yebo Wu, and Cheng-Zhong Xu. 2024. Breaking the Memory Wall for Heterogeneous Federated Learning via Model Splitting. *IEEE Transactions on Parallel and Distributed Systems* (2024).
- [54] Taegeon Um, Byungsoo Oh, Minyoung Kang, Woo-Yeon Lee, Goeun Kim, Dongseob Kim, Youngtaek Kim, Mohd Muzzammil, and Myeong-jae Jeon. 2024. Metis: Fast Automatic Distributed Training on Heterogeneous {GPUs}. In *2024 USENIX Annual Technical Conference (USENIX ATC 24)*. 563–578.
- [55] Ashish Vaswani, Noam Shazeer, Niki Parmar, Jakob Uszkoreit, Llion Jones, Aidan N. Gomez, Lukasz Kaiser, and Illia Polosukhin. 2023. Attention Is All You Need. arXiv:1706.03762 [cs]
- [56] Kun Wang, Jiani Cao, Zimu Zhou, and Zhenjiang Li. 2024. SwapNet: Efficient Swapping for DNN Inference on Edge AI Devices Beyond the Memory Budget. *IEEE Transactions on Mobile Computing* (2024).
- [57] Yousuke Watanabe, Kenya Sato, and Hiroaki Takada. 2020. DynamicMap 2.0: A Traffic Data Management Platform Leveraging Clouds, Edges and Embedded Systems. *International Journal of Intelligent Transportation Systems Research* 18, 1 (2020), 77–89. <https://doi.org/10.1007/s13177-018-0173-7>
- [58] Qizhen Weng, Wencong Xiao, Yinghao Yu, Wei Wang, Cheng Wang, Jian He, Yong Li, Liping Zhang, Wei Lin, and Yu Ding. 2022. {MLaaS} in the Wild: Workload Analysis and Scheduling in {Large-Scale} Heterogeneous {GPU} Clusters. In *19th USENIX Symposium on Networked Systems Design and Implementation (NSDI 22)*. 945–960.
- [59] wikipedia. 2025. Local Area Network. *Wikipedia* (2025).
- [60] Tengxi Xia, Ju Ren, Wei Rao, Qin Zu, Wenjie Wang, Shuai Chen, and Yaoyue Zhang. 2024. Aerorec: An Efficient on-Device Recommendation Framework Using Federated Self-Supervised Knowledge Distillation. In *IEEE INFOCOM 2024-IEEE Conference on Computer Communications*. IEEE, 121–130.
- [61] Daliang Xu, Mengwei Xu, Chiheng Lou, Li Zhang, Gang Huang, Xin Jin, and Xuanzhe Liu. 2024. SoCFlow: Efficient and Scalable DNN Training on SoC-Clustered Edge Servers. In *Proceedings of the 29th ACM International Conference on Architectural Support for Programming Languages and Operating Systems, Volume 1*. ACM, La Jolla CA USA, 368–385. <https://doi.org/10.1145/3617232.3624847>
- [62] Enyue Yang, Weike Pan, Qiang Yang, and Zhong Ming. 2024. Discrete Federated Multi-behavior Recommendation for Privacy-Preserving Heterogeneous One-Class Collaborative Filtering. *ACM Transactions on Information Systems* 42, 5 (2024), 1–50.
- [63] Lei Yang, Yingqi Gan, Jinru Chen, and Jiannong Cao. 2024. AutoSF: Adaptive Distributed Model Training in Dynamic Edge Computing. *IEEE Transactions on Mobile Computing* 23, 6 (2024), 6549–6562. <https://doi.org/10.1109/TMC.2023.3323456>
- [64] Shengyuan Ye, Liekang Zeng, Xiaowen Chu, Guoliang Xing, and Xu Chen. 2024. Asteroid: Resource-Efficient Hybrid Pipeline Parallelism for Collaborative DNN Training on Heterogeneous Edge Devices. In *Proceedings of the 30th Annual International Conference on Mobile Computing and Networking (ACM MobiCom '24)*. Association for Computing Machinery, New York, NY, USA, 312–326. <https://doi.org/10.1145/3636534.3649363>
- [65] Liekang Zeng, Xu Chen, Zhi Zhou, Lei Yang, and Junshan Zhang. 2021. CoEdge: Cooperative DNN Inference With Adaptive Workload Partitioning Over Heterogeneous Edge Devices. *IEEE/ACM Transactions on Networking* 29, 2 (April 2021), 595–608. <https://doi.org/10.1109/TNET.2020.3042320>
- [66] Mingshu Zhai, Jiaao He, Zixuan Ma, Zan Zong, Runqing Zhang, and Jidong Zhai. 2023. {SmartMoE}: Efficiently Training {Sparsely-Activated} Models through Combining Offline and Online Parallelization. In *2023 USENIX Annual Technical Conference (USENIX ATC 23)*. 961–975.
- [67] Haotong Zhang, Weiwei Lin, Rong Xie, Shenghai Li, Zhiyan Dai, and James Z. Wang. 2024. An Optimal Container Update Method for Edge-cloud Collaboration. *Software: Practice and Experience* 54, 4 (2024), 617–634. <https://doi.org/10.1002/spe.3232>
- [68] Lizhi Zhang, Kai Lu, Zhiquan Lai, Yongquan Fu, Yu Tang, and Dongsheng Li. 2023. Accelerating GNN Training by Adapting Large Graphs to Distributed Heterogeneous Architectures. *IEEE Trans. Comput.* 72, 12 (2023), 3473–3488. <https://doi.org/10.1109/TC.2023.3305077>
- [69] Shijin Zhang, Zidong Du, Lei Zhang, Huiying Lan, Shaoli Liu, Ling Li, Qi Guo, Tianshi Chen, and Yunji Chen. 2016. Cambricon-X: An Accelerator for Sparse Neural Networks. In *2016 49th Annual IEEE/ACM International Symposium on Microarchitecture (MICRO)*. IEEE, 1–12.
- [70] Siyao Zhang, Daocheng Fu, Wenzhe Liang, Zhao Zhang, Bin Yu, Pinlong Cai, and Baozhen Yao. 2024. Trafficgpt: Viewing, Processing and Interacting with Traffic Foundation Models. *Transport Policy* 150 (2024), 95–105.
- [71] Weigang Zhang, Biyu Zhou, Xuehai Tang, Zhaoxing Wang, and Songlin Hu. 2023. MixPipe: Efficient Bidirectional Pipeline Parallelism for Training Large-Scale Models. In *2023 60th ACM/IEEE Design Automation Conference (DAC)*. 1–6. <https://doi.org/10.1109/DAC56929.2023.10247730>
- [72] Yanli Zhao, Andrew Gu, Rohan Varma, Liang Luo, Chien-Chin Huang, Min Xu, Less Wright, Hamid Shojanazeri, Mye Ott, Sam Shleifer, Alban Desmaison, Can Balioglu, Pritam Damania, Bernard Nguyen, Geeta Chauhan, Yuchen Hao, Ajit Mathews, and Shen Li. 2023. PyTorch FSDP: Experiences on Scaling Fully Sharded Data Parallel. *Proceedings of the VLDB Endowment* 16, 12 (Aug. 2023), 3848–3860. <https://doi.org/10.14778/3611540.3611569>
- [73] Zhuoran Zhao, Kamyar Mirzazad Barijough, and Andreas Gerstlauer. 2018. DeepThings: Distributed Adaptive Deep Learning Inference on Resource-Constrained IoT Edge Clusters. *IEEE Transactions on Computer-Aided Design of Integrated Circuits and Systems* 37, 11 (2018), 2348–2359. <https://doi.org/10.1109/TCAD.2018.2858384>
- [74] Lianmin Zheng, Zhuohan Li, Hao Zhang, Yonghao Zhuang, Zhifeng Chen, Yanping Huang, Yida Wang, Yanzhong Xu, Danyang Zhuo, Eric P. Xing, Joseph E. Gonzalez, and Ion Stoica. 2022. Alpa: Automating Inter- and Intra-Operator Parallelism for Distributed Deep Learning. In *16th USENIX Symposium on Operating Systems Design and Implementation (OSDI 22)*. 559–578.
- [75] Ruiqi Zheng, Liang Qu, Tong Chen, Kai Zheng, Yuhui Shi, and Hongzhi Yin. 2024. Personalized Elastic Embedding Learning for On-Device Recommendation. *IEEE Transactions on Knowledge and Data Engineering* (2024).
- [76] Yinmin Zhong, Zili Zhang, Xiaoni Song, Hanpeng Hu, Chao Jin, Bingyang Wu, Nuo Chen, Yukun Chen, Yu Zhou, Changyi Wan, Hongyu Zhou, Yimin Jiang, Yibo Zhu, and Daxin Jiang. 2025. StreamRL:

Scalable, Heterogeneous, and Elastic RL for LLMs with Disaggregated Stream Generation. <https://doi.org/10.48550/arXiv.2504.15930> arXiv:2504.15930 [cs]

[77] Jiahang Zhou, Yanyu Chen, Zicong Hong, Wuhui Chen, Yue Yu, Tao Zhang, Hui Wang, Chuanfu Zhang, and Zibin Zheng. 2024. Training

and Serving System of Foundation Models: A Comprehensive Survey. arXiv:2401.02643 [cs]

Received 20 February 2007; revised 12 March 2009; accepted 5 June 2009